Pyridine *N*-Oxides Catalyzed Living Radical Polymerization of Methacrylates via Halogen Bonding Catalysis

*Haiyan Xu, Chen-Gang Wang, Yunpeng Lu, and Atsushi Goto**

Division of Chemistry and Biological Chemistry, School of Physical and Mathematical Sciences, Nanyang Technological University, 21 Nanyang Link, 637371, Singapore

KEYWORDS: pyridine *N*-oxides, halogen bonding, living radical polymerization, functional methacrylates, block polymers

ABSTRACT: The paper reports the generation of a carbon-center radical ($R^{\bullet}$) from an alkyl iodide (R-I) via a halogen bonding catalysis using pyridine *N*-oxide (PO) catalysts. The use of this catalysis in organocatalyzed living radical polymerization was systematically studied over a series of substituted POs. A more electron-donating substitute led to a higher catalytic activity, as experimentally observed and theoretically supported by DFT (density functional theory) calcuation. Notably, the polymerization was induced and controlled not only by thermal heating but also photo irradiation. The polymerization was compatible with several functional monomers and afforded block copolymers.

INTRODUCTION

Halogen bonding (R–X···Y) is a non-covalent interaction between an electron-accepting halogen (X) and an electron-donating group (Y).[1,2] The strength of the interaction depends on X and Y. Halogen bonding has attracted attention in crystal engineering[3] and supramolecular chemistry.[4,5]

Our research group was the first to utilize a halogen bonding of an alkyl iodide (R−I) and an organic catalyst (Y) to reversibly generate the alkyl radical ($R^{\bullet}$) from R−I.[6-11] Exploiting this novel organocatalysis, we developed an organocatalyzed living radical polymerization that uses an R–I as an initiator (initiating dormant species) and an organic molecule as a catalyst (Scheme 1a). Living radical polymerization is a powerful method for synthesizing polymers with predictable molecular weights, narrow molecular-weight distributions, and well-defined structures.[12-23]

The catalysts in the organocatalyzed polymerization included tertiary amines,[7] iodide anion (I^-),[8,9,11] and azido anion (N_3^-).[10] The dormant species (polymer–I) and the catalyst are supposed to form a halogen-bonding complex (polymer–I···catalyst). The complex subsequently reversibly generates the propagating radical (polymer$^{\bullet}$) (Scheme 1a). We term this polymerization reversible complexation mediated polymerization (RCMP).[7,8] Attractive features of RCMP include the use of inexpensive compounds, ease of operation, and applicability to a range of polymer design, which are beneficial in practical applications. Among the mentioned catalysts, the ionic catalysts (I^- and N_3^-) exhibited much higher catalytic activities than the neutral amines, because of the higher electro-donating ability of I^- and N_3^-. However, owing to no substituent on

these anions (I^- and N_3^-), there is no possibility to manipulate their catalytic activities electronically or sterically.

Based on this background, in the present work, we employed ionic pyridine *N*-oxide ($C_5H_5N^+$-O^-) (PO) and its substituted derivatives as catalysts (Schemes 1b and 1c). PO catalysts are ionic, and the O^- moiety can coordinate iodide.[24-26] The catalytic activity is able to tune by altering the substituents of PO, which is a unique feature of PO catalysts over the previous ionic catalysts. PO catalysts are also more favourable in practical application for their good solubility in non-polar monomers, whereas the previous ionic catalysts have limited solubilities in non-polar monomers.

Herein, we report a systematic study on the use of various PO derivatives (Schemes 1c) as RCMP catalysts. This is the first halogen bonding catalysis using PO and its derivatives to generate $R^\bullet$ from R−I in organic chemistry. The systematic study revealed significant effects of the substituents on this catalysis. Synthetically, PO is attractive for its ease of derivatization, enabling tailored design of the catalysts with different catalytic activities and solubilities. A further notable aspect is that the polymerization can be induced and controlled not only by thermal heating but also photo irradiation, as will be described below.

Scheme 1. (a) Reversible Activation in RCMP, (b) Synthesis of Polymer, and (c) Structures and Abbreviations of Studied Catalysts and Results of MMA Polymerizations.

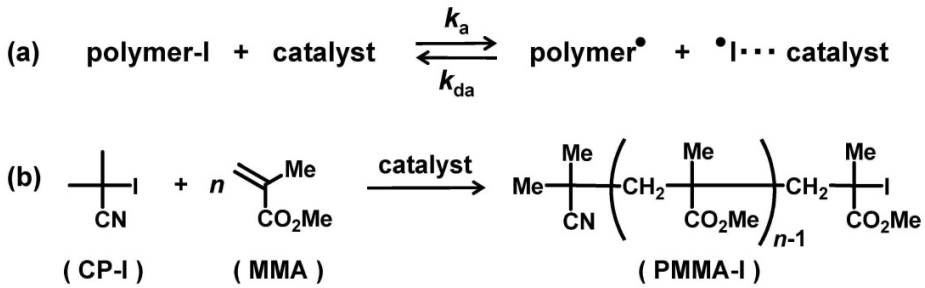

(c) $[MMA]_0/[CP\text{-}I]_0/[catalyst]_0/[I_2]_0$ = 8000/80/20/1 (70 °C, 12 h)

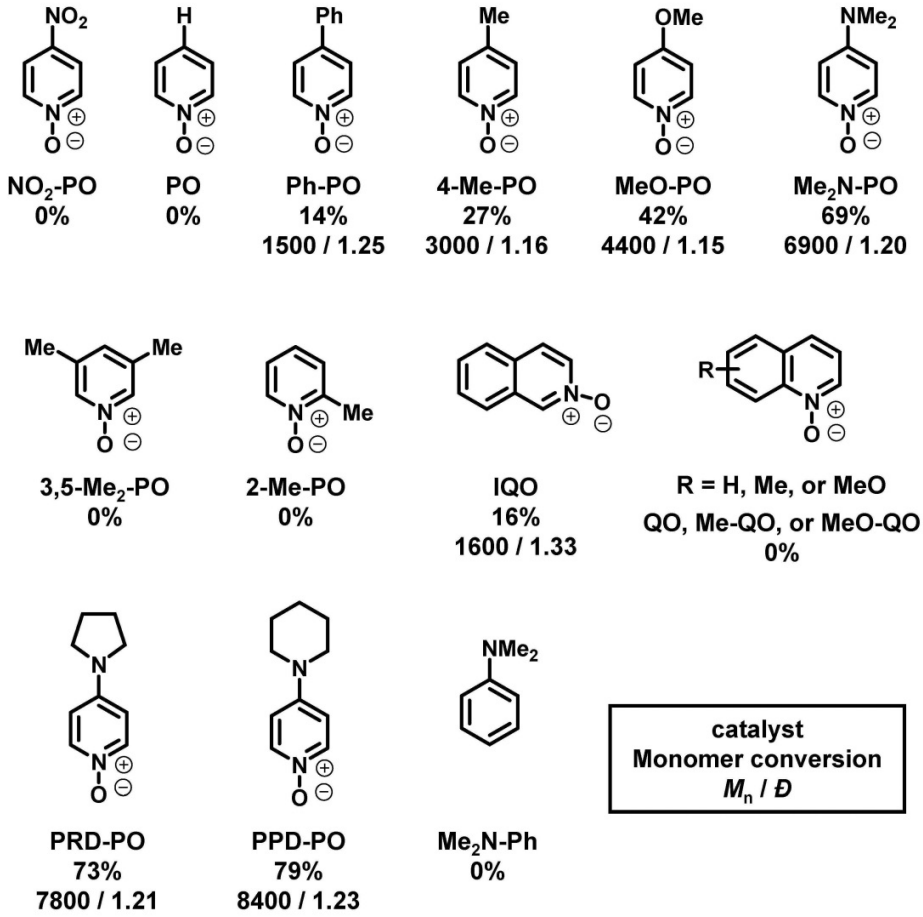

RESULTS AND DISCUSSION

Experimental Proof of the Generation of R$^{\bullet}$ from R−I with a Substituted PO Catalyst. A radical trap experiment[8,27] was performed to demonstrate the generation of R$^{\bullet}$ from R−I using 4-methoxypyridine *N*-oxide (MeO−PO, Scheme 1c). We heated 2-iodo-2-methylpropionitrile (CP−I, Scheme 1b, 20 mM) as an R−I, MeO−PO (20 mM) as a catalyst, and 2,2,6,6-tetramethylpiperidine-1-oxyl (TEMPO, 80 mM) as a radical trap in a mixture of toluene-d_8 (90%) and acetonitrile-d_3 (10%) at 70 ^{o}C. The mixture of toluene-d_8 (dielectric constant ε = 2.4) and acetonitrile-d_3 (ε = 37.5) is a model of methyl methacrylate (MMA) medium (ε = 7.9). If CP−I reacts with MeO−PO, the generated radical CP$^{\bullet}$ is trapped by TEMPO, thereby yielding CP−TEMPO. Figure 1 shows the ^{1}H NMR spectra of the reaction mixture. After 1 h, new peaks appeared and matched those of the pure CP−TEMPO independently prepared. After 5 h, the extent of the reaction of CP−I to CP−TEMPO was 85% with an error range of 80-90%. Because MeO−PO is a (weak) base, it can promote the elimination of HI from CP−I as a side reaction. In the studied case, 15% of the elimination product (methacrylonitrile) was observed for 5 h (Figure 1). These results clearly demonstrate the generation of R$^{\bullet}$ from R−I using MeO−PO, which is a main reaction, and also show a presence of the elimination reaction as a side reaction. In the absence of TEMPO, the reaction was reversible. Exploiting the reversible nature, we utilized PO and its derivatives as catalysts for RCMP.

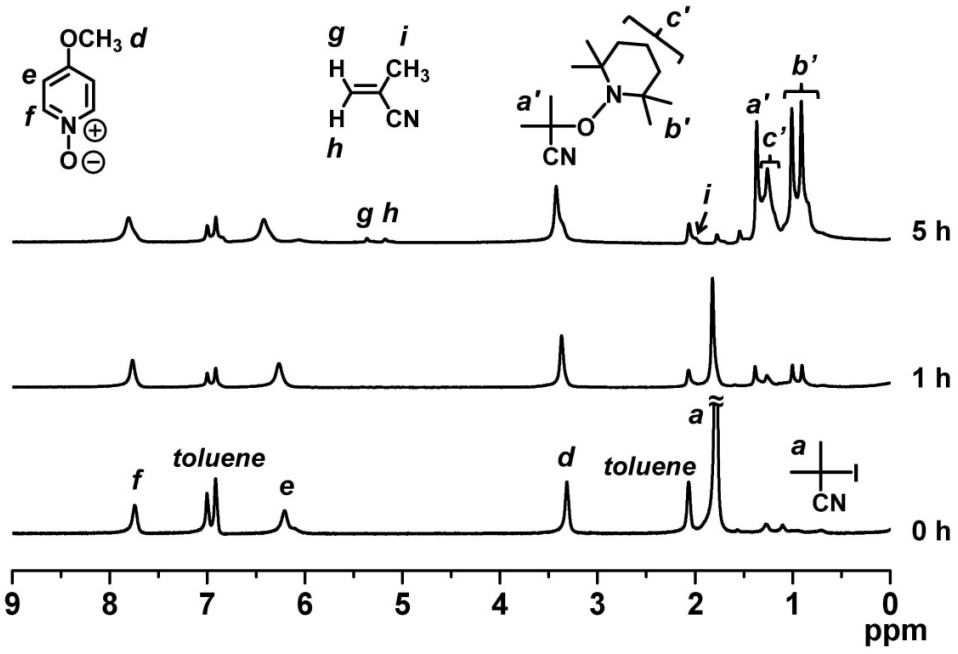

Figure 1. ^{1}H NMR (300 MHz) spectra of the solution of CP-I (20 mM), MeO-PO (20 mM), and TEMPO (80 mM) heated at 70 ^{o}C for 0, 1, and 5 h. The solvent was a mixture of toluene–d_8 and acetonitrile-d_3 (9/1).

Polymerizations of MMA with a Series of Substituted PO Catalysts. Table 1 (entries 1-14) and Scheme 1c summarize the results of the polymerizations of MMA using various PO catalysts. A mixture of MMA (monomer) (90 wt%, 8 M), CP–I (initiating dormant species, 80 mM), a catalyst (20 mM), and I_2 (1 mM) in toluene (10 wt%) was heated at 70 °C for 12 h. Scheme 1c shows the structures and abbreviations of the studied PO catalysts and the number-average molecular weight (M_n) and dispersity ($Đ = M_w/M_n$) of the obtained polymer, where M_w is the weight-average molecular weight. Toluene was added for better solubility of the PO catalysts. I_2 was added to increase the deactivation rate and thereby lower the $Đ$ value.

For *para*-substituted POs (Table 1 (entries 1-6) and the first line in Scheme 1c), the monomer conversion (for 12 h) increased in the order of nitro (0%) ~ hydrogen (0%) < phenyl (14%) <

methyl (27%) < methoxy (42%) < dimethylamino (69%) substituents. As a clear trend, a stronger electron-donating substituent brought a higher catalytic activity because of the increased electron density on the O^- moiety and the thereby enhanced halogen bonding. With phenyl, methyl, methoxy, and dimethylamino-substituted POs, the M_n value agreed well with the theoretical value (calculated with $[MMA]_0$, $[CP–I]_0$, and monomer conversion) (Table 1 (entries 3-6)), and the $Đ$ value was as low as 1.15-1.25, demonstrating a good control of polymerization.

The orientation of the substituent was important. For the methyl substituent, while the *para*-substituted PO (4-Me-PO) gave 27% monomer conversion for 12 h (Table 1 (entry 4)), the *meta*- and *ortho*-substituted POs (3,5-Me_2-PO and 2-Me-PO) gave no polymerization (Table 1 (entries 7 and 8)). This would be because the *meta*-orientation is less effective to increase the electron density of the O^- moiety (electronic effect) and the *ortho*-substitution gives steric hindrance at the O^- moiety (steric effect). Quinoline oxides with extended aromaticity (IQO, QO, Me-QO, and MeO-QO) led to less catalytic activities than POs due to the delocalization of the electron (less electron density on the O^- moiety) (Table 1 (entries 9-12) and Scheme 1c).

Table 1. Polymerizations of MMA.

Entry	Catalyst	Target DP[a]	$[MMA]_0/[CP\text{-}I]_0/[catalyst]_0/[V65]_0/[I_2]_0$ (mM)[b]	T (°C)	t (h)	Conv (%)	M_n ($M_{n,theo}$[c])	$Đ$
1	NO_2-PO	100	8000/80/20/0/1	70	12	0	–	–
2	PO	100	8000/80/20/0/1	70	12	0	–	–
3	Ph-PO	100	8000/80/20/0/1	70	12	14	1500 (1400)	1.25
4	4-Me-PO	100	8000/80/20/0/1	70	12	27	3000 (2700)	1.16
5	MeO-PO	100	8000/80/20/0/1	70	12	42	4400 (4200)	1.15
6	Me_2N-PO	100	8000/80/20/0/1	70	12	69	6900 (6900)	1.20
7	3,5-Me_2-PO	100	8000/80/20/0/1	70	12	0	–	–
8	2-Me-PO	100	8000/80/20/0/1	70	12	0	–	–
9	IQO	100	8000/80/20/0/1	70	12	16	1600 (1600)	1.33
10	QO	100	8000/80/20/0/1	70	12	0	–	–
11	Me-QO	100	8000/80/20/0/1	70	12	0	–	–
12	MeO-QO	100	8000/80/20/0/1	70	12	0	–	–
13	PRD-PO	100	8000/80/20/0/1	70	12	73	7800 (7300)	1.21
14	PPD-PO	100	8000/80/20/0/1	70	12	79	8400 (7900)	1.23
15	Me_2N-Ph	100	8000/80/20/0/1	70	12	0	–	–
16	PPD-PO	100	8000/80/20/5/1	60	6	90	9200 (9000)	1.15
17	PPD-PO	200	8000/40/20/5/1	60	5	90	18200 (18000)	1.29
18	PPD-PO	400	8000/20/20/5/1	60	5	83	35000 (33000)	1.39
19	PPD-PO	100	8000/80/20/0/0 (photo irradiation)	rt	10	79	7900 (7900)	1.09
20	PPD-PO	200	8000/40/20/0/0 (photo irradiation)	rt	11	76	15000 (15000)	1.12
21	PPD-PO	400	8000/20/20/0/0 (photo irradiation)	rt	12	66	28000 (26000)	1.20
22	PPD-PO	100	8000/80/20/0/0 (photo irradiation)	rt	2 h × 5	84	8400 (8400)	1.23
23	none	100	8000/80/0/0/0 (photo irradiation)	rt	10	0	–	–
24	PPD-PO	30	8000/267/20/0/1	70	3.5	63	1800[d] (1900)	1.12[d]
25	PPD-PO	30	8000/267/20/0/0 (photo irradiation)	rt	3.5	55	2000[d] (1700)	1.16[d]

[a]Target degree of polymerization (DP) at 100% monomer conversion (calculated by $[MMA]_0/[CP{-}I]_0$). [b]Addition of 10 wt% toluene (90 wt% monomer). [c]Theoretical M_n calculated with $[monomer]_0$, $[CP{-}I]_0$, and monomer conversion. [d]After purification (for the subsequent ^1H NMR analysis).

Among the mentioned 12 catalysts, the dimethylamino-substituted PO, i.e., 4-dimethylaminopyridine *N*-oxide (Me_2N-PO) (Table 1 (entry 6) and Scheme 1c), exhibited the highest catalytic activity. This result motivated us to study cyclic dialkylamino-POs, i.e., 4-(pyrrolidin-1-yl)pyridine *N*-oxide (PRD-PO) and 4-(piperidin-1-yl)pyridine *N*-oxide (PPD-PO) (Table 1 (entries 13 and 14) and Scheme 1c). PRD-PO and PPD-PO are not commercially available but were easily synthesized via a one-step reaction of 4-chloro-PO with pyrrolidine or piperidine with a good yield (90%) (Supporting Information).[28] The ease of their synthesis is an attractive aspect for extensive use. Figure 2 (filled symbols) shows the full polymerization behaviours for the three catalysts (Me_2N-PO, PRD-PO, and PPD-PO). These catalysts showed similar polymerization rates, as the monomer conversion reached 69-79% in 12 h. In all cases, the M_n values agreed well with the theoretical values and the $Đ$ values were small (approximately 1.2) from an early stage of polymerization, indicating a sufficiently fast activation (catalytic) process (Scheme 1a). It should be noted that the six-membered PPD-PO is readily dissolved in non-polar monomers and showed a superior solubility compared with the previous ionic catalysts (I^- and N_3^-).

The experimentally observed higher catalytic activity of PPD-PO than that of the non-substituted PO was supported by density functional theory (DFT) calculation (Scheme 2). We calculated the Gibbs free energy change (ΔG) from the reactants (MMA-I and catalyst) to the corresponding products ($MMA^\bullet$ and catalyst$\cdots I^\bullet$), where MMA-I is methyl 2-iodo-2-methylpropionate as a model of polymethacrylate-iodide. The ΔG value was much smaller for PPD-PO (116.1 kJ/mol) than that of PO (128.3 kJ/mol), being consistent with the experimental result.

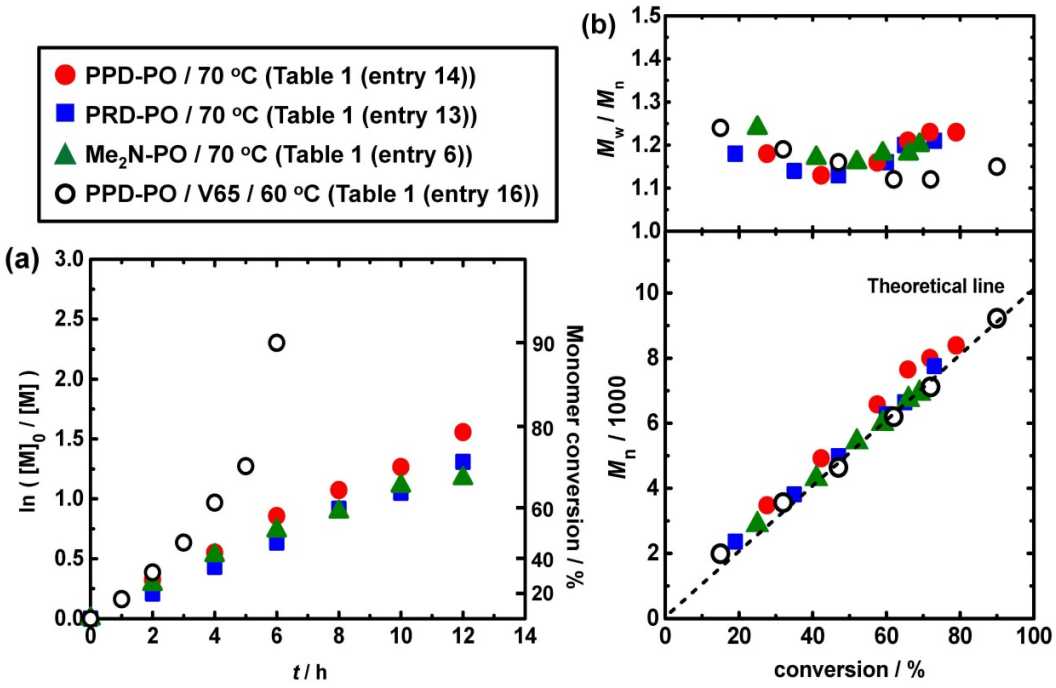

Figure 2. Plots of (a) ln([M]$_0$/[M]) vs t and (b) M_n and M_w/M_n vs conversion for the MMA/CP-I/catalyst/I$_2$/(V65) systems (70 or 60 °C): [MMA]$_0$ = 8 M; [CP-I]$_0$ = 80 mM; [catalyst]$_0$ = 20 mM; [I$_2$]$_0$ = 1 mM; [V65]$_0$ = 0 or 5 mM in toluene (10 wt%). The symbols are indicated in the figure. The experimental conditions are given in Table 1 (entries 6, 13, 14, and 16).

Scheme 2. Gibbs Free Energy Change for Reactions of MMA-I with PO and PPD-PO.

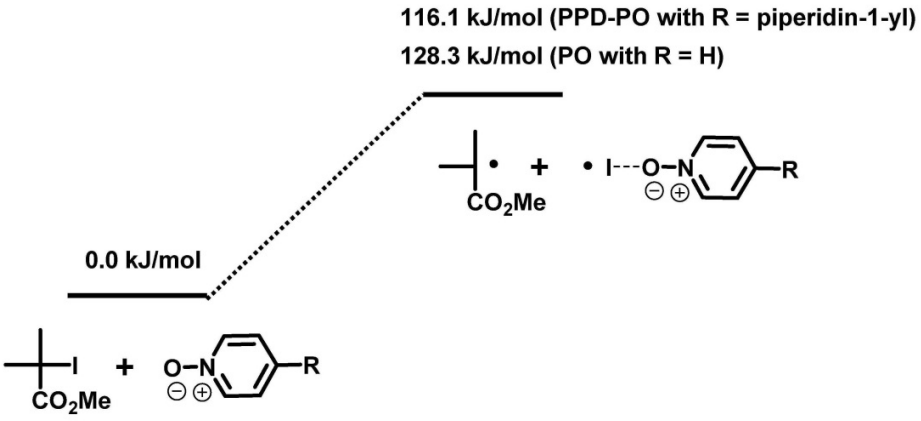

In the previous study, neutral tertiary amines such as tributylamine were used as effective catalysts.[7] Because Me_2N-PO, PRD-PO, and PPD-PO also contain a tertiary amine as well as a PO moiety, we studied their reference compound without the PO moiety, i.e., dimethyl aniline (Me_2N-Ph) (Table 1 (entry 15) and Scheme 1c). No polymerization took place with the reference compound, meaning that the catalytic site of the three PO catalysts is the O^- moiety. The previously studied tributylamine contains three alkyl groups, while Me_2N-Ph contains two alkyl groups and an aromatic group. The aromatic group delocalizes electrons and reduces the electron density of the amine moiety, which would lead to no catalytic activity of Me_2N-Ph.

Increase in the Polymerization Rate and Higher Molecular Weights. While PPD-PO was an efficient catalyst, the polymerization rate (R_p) was rather low; namely, the monomer conversion reached 79% after a relatively long time of 12 h at 70 °C (Table 1 (entry 14) and Figure 2, filled circles). An effective way to overcome the slow polymerization was the addition of a small amount of an azo initiator, 2,2'-azobis(2,4-dimethylvaleronitrile) (V65) (Table 1 (entry 16) and Figure 2, open circles). Azo initiators are often used to decrease the deactivator concentration and hence effectively increase R_p in other living radical polymerizations.[23,29] As Figure 2 shows, the addition of V65 (5 mM) dramatically increased R_p even at a lower temperature of 60 °C. The addition of a small amount of V65 did not significantly affect M_n or $Đ$ despite the significant increase in R_p. The monomer conversion reached 90% in a relatively short time of 6 h at the mild temperature of 60 °C. The accelerated polymerization rate at the later stage of polymerization (Figure 2, open circles) is ascribed to the gel effect (high viscosity). The small $Đ$ values achievable at high conversions are highly attractive in practical use. Higher degrees of polymerization (DPs) were also attained. We targeted DPs of 200 and 400 at 100% monomer conversion and obtained low-dispersity ($Đ$ = 1.29–1.39) polymers with high monomer

conversions (83–90%) in a reasonably short reaction time (5 h) up to M_n of 35,000 (Table 1 (entries 17 and 18)).

Toluene was used as a solvent in the polymerizations. To check if the halogen bonding is affected by the solvent, we carried out an experiment using an ester solvent, i.e., ethyl acetate, which is structurally more close to MMA. Similar results were obtained with the use of toluene (entry 16 in Table 1) (monomer conversion = 90%, M_n = 9200, $Đ$ = 1.15 for 6 h) and the use of ethyl acetate (monomer conversion = 93%, M_n = 11300, $Đ$ = 1.26 for 6 h) in the same condition but using the different solvents. These results suggest that the halogen bonding is not affected by these solvents. We used a small amount of I_2 (entry 16 in Table 1). Compared with the system with I_2, the absence of I_2 resulted in a higher polymerization rate and a slightly higher $Đ$ value (monomer conversion = 92%, M_n = 9200, $Đ$ = 1.20 for 5 h (not 6 h)), as expected.

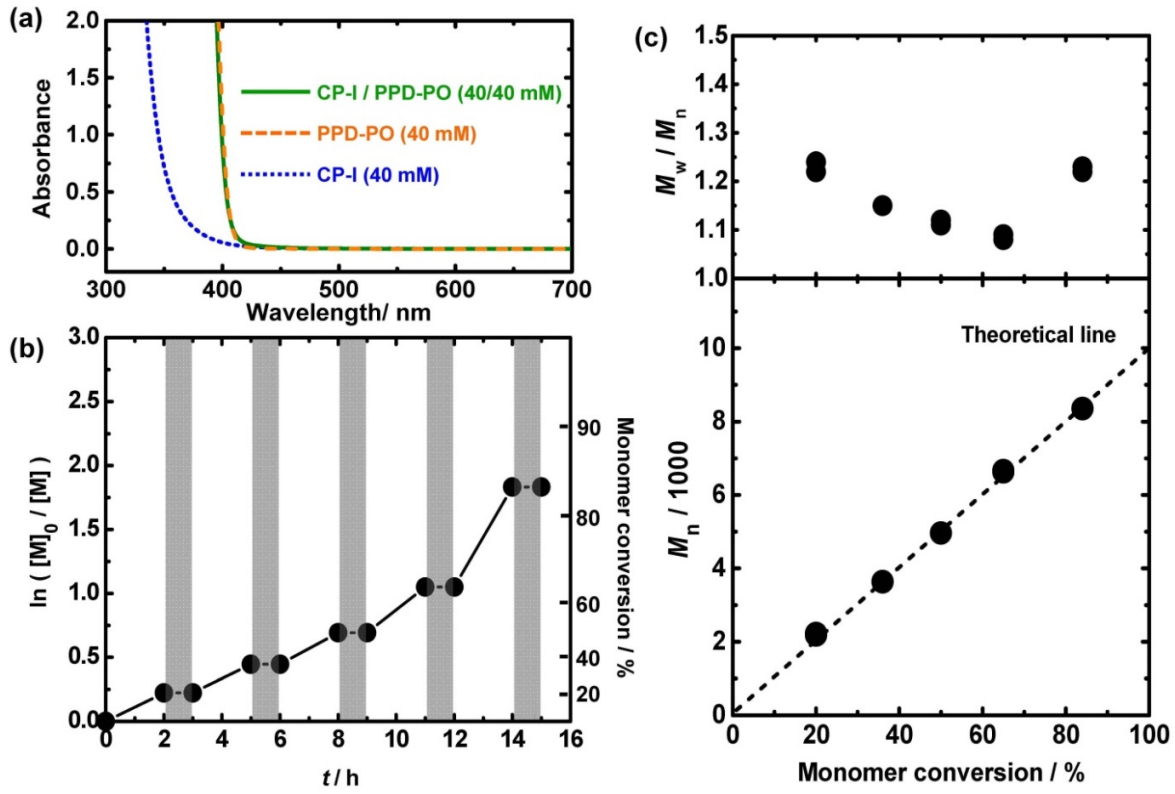

Figure 3. (a) UV-vis spectra of pure CP-I (blue dotted line), pure PPD-PO (orange dashed line), and a mixture of CP-I and PPD-PO (green solid line) in MMA. (b) Plot of ln([M]$_0$/[M]) vs t for the MMA/CP-I/PPD-PO system (room temperature): [MMA]$_0$ = 8 M; [CP-I]$_0$ = 80 mM; [PPD-PO]$_0$ = 20 mM in toluene (10 wt% of MMA). (c). Plots of M_n and M_w/M_n vs monomer conversion for the same system.

Photo Polymerizations. The polymerization was able to control by not only thermal heating but also photo irradiation (Figure 3 and Table 1 (entries 19-22)). The halogen bonding complex (polymer–I···catalyst) photochemically dissociates to generate polymer$^{\bullet}$. Figure 3a shows the absorption spectra of pure CP-I (blue dotted line), pure PPD-PO (orange dashed line), and a mixture of CP-I and PPD-PO (green solid line), where the medium was MMA in all cases. Pure PPD-PO and the mixture of CP-I and PPD-PO showed almost identical absorption spectra tailing to 430 nm. No distinct peak for the complex (CP–I···PPD-PO) was observed, indicating that the complex has a similar absorption to that of pure PPD-PO in this particular case.

We carried out the polymerization of MMA (8 M, 100 eq) with CP-I (80 mM, 1 eq) and PPD-PO (20 mM, 0.25 eq) under LED (light emitting diode) irradiation (380-550 nm) at ambient temperature (20 ^{o}C). Figures 3b and 3c and Table 1 (entry 22) demonstrate the temporal control of the polymerization. The LED light was turned on for 2 h and off for 1 h in a repetitive manner for five cycles. When the light was turned on, the system was switched "on" and the polymerization smoothly proceeded in all cycles. When the light was turned off, the system was immediately switched "off" and perfectly no polymerization occurred in the dark. The M_n and dispersity were also well controlled. This system is an excellent photo-switchable polymerization. Without a catalyst (PPD-PO), no polymerization took place under the irradiation (Table 1 (entry 23)). Under continuous irradiation, we obtained low-dispersity ($Đ$ = 1.09–1.20) polymers with M_n up to 28000 using the PPD-PO catalyst (Table 1 (entries 19-21)). Other PO catalysts were also effective for the photo polymerizations of MMA (Supporting Information (Figure S5)).

Chain-End Fidelity. Using ^{1}H NMR (Supporting Information (Figures S6 and S7)),[30] we analysed the chain-end of the PMMAs obtained in a thermal condition (M_n = 1800 and $Đ$ = 1.12 after purification (Table 1 (entry 24) with monomer conversion = 63%)) and a photo condition (M_n = 2000 and $Đ$ = 1.16 after purification (Table 1 (entry 25) with monomer conversion = 55%)), where PMMA is poly(methyl methacrylate). The polymer obtained in the thermal condition possessed 59% iodide and 41% lactone at the growing chain end (with ± 5% experimental error). The lactone chain end is generated via an ionic side reaction.[31] (The small $Đ$ value (1.12) of this polymer indicates that the accumulation of the lactone chain end polymer was significant at a later stage of polymerization.) In contrast, the polymer obtained in the photo condition possessed 98% iodide with an error range of 93-100%. The side reaction was significantly suppressed probably because of the decreased temperature (70 ^{o}C and 20 ^{o}C for the

thermal and photo conditions, respectively). These results demonstrate moderate and almost quantitative iodide-chain-end fidelty in the thermal and photo conditions, respectively.

Table 2. Polymerizations of Functional Methacrylates Using PPD-PO.

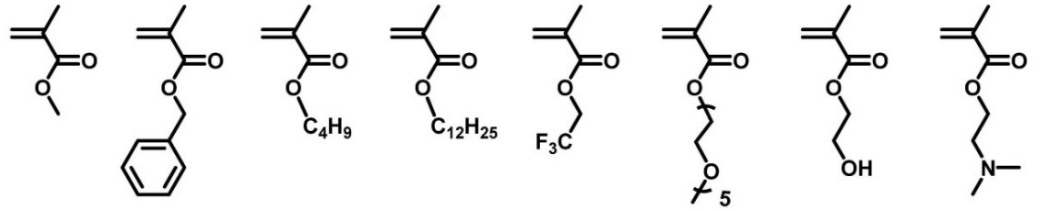

Entry	Monomer[a]	R-I	Target DP[b]	$[M]_0/[R\text{-}I]_0/[PPD\text{-}PO]_0/[V65]_0/[I_2]_0$ (mM)[c]	T (^oC)	t (h)	Conv (%)	M_n[d] ($M_{n,theo}$[e])	$Đ$[d]
1	BzMA	CP-I	100	8000/80/20/5/1	70	4	95	16000 (17000)	1.15
2	BMA	CP-I	100	8000/80/20/5/0	60	7	80	10000 (11000)	1.35
3	LMA	CP-I	100	8000/80/20/5/0	60	10	82	18000 (21000)	1.29
4	TFEMA	CP-I	100	8000/80/20/5/0	60	8	80	12000 (13000)	1.32
5	PEGMA[f]	CP-I	100	8000/80/20/20/0	50	9	87	27000 (26000)	1.40
6	HEMA	CP-I	100	8000/80/80/20/1	50	1.5	84	36000 (11000)	1.49
7	DMAEMA	CP-I	100	8000/80/20/5/0	50	12	86	9200 (14000)	1.46
8	BzMA	PMMA-I[g]	50	8000/160/20/5/1	70	3.5	84	10000 (12000)	1.16
9	PEGMA	PMMA-I[h]	50	8000/160/20/40/1	50	10	64	13000 (14000)	1.21
10	MMA	PPEGMA-I[i]	100	8000/80/20/5/1	70	4	86	32000 (29000)	1.36

[a]BzMA = benzyl methacrylate, BMA = butyl methacrylate, LMA = lauryl methacrylate, TFEMA = 2,2,2-trifluoroethyl methacrylate, PEGMA = poly(ethylene glycol) methyl ether methacrylate, HEMA = 2-hydroxyethyl methacrylate, and DMAEMA = (dimethylamino)ethyl methacrylate. [b]Target degree of polymerization (DP) at 100% monomer conversion (calculated by $[monomer]_0/[R{-}I]_0$). [c]Addition of 10 wt% toluene (90 wt% monomer) for entries 1-5 and 7-10 and no addition of solvent (in bulk) for entry 6. [d]PMMA-calibrated GPC values. [e]Theoretical M_n calculated with $[monomer]_0$, $[R{-}I]_0$, and monomer conversion. [f]Molecular weight of monomer = 300. [g]PMMA-I is poly(methyl methacrylate)-iodide with M_n = 4700 and $Đ$ = 1.09. [h]PMMA-I with M_n = 4200 and $Đ$ = 1.10. [i]PPEGMA-I is poly(poly(ethylene glycol) methyl ether methacrylate)-iodide with M_n = 20000 and $Đ$ = 1.21.

Table 3. Photo Polymerizations of Functional Methacrylates Using PPD-PO.[a]

Entry	Monomer[b]	R-I	Target DP[c]	$[Monomer]_0/[R\text{-}I]_0/[PPD\text{-}PO]_0/[I_2]_0$ (mM)[d]	t (h)	Conv (%)	M_n[e] ($M_{n,theo}$[f])	$Đ$[e]
1	BzMA	CP-I	100	8000/80/20/0	7	83	14000 (15000)	1.15
2	BMA	CP-I	100	8000/80/20/0	9	93	13000 (13000)	1.13
3	TFEMA	CP-I	100	8000/80/20/0	10	75	13000 (13000)	1.21
4	PEGMA[g]	CP-I	100	8000/80/20/0	10	91	29000 (27000)	1.22
5	HEMA	CP-I	100	8000/80/80/1	4	70	19000 (9100)	1.43
6	DMAEMA	CP-I	100	8000/80/20/0	7	90	13000 (14000)	1.17
7	BzMA	PMMA-I[h]	50	8000/160/20/0	10	82	8800 (9100)	1.10
8	DMAEMA	PMMA-I[i]	50	8000/160/20/0	7	77	8000 (9500)	1.18
9	MMA	PPEGMA-I[j]	100	8000/80/20/0	5	91	24000 (25000)	1.28
10	DMAEMA	PPEGMA-I[j]	100	8000/80/20/0	5	86	27000 (29000)	1.33

[a]LED irradiation (380-550 nm) at ambient temperature (20 °C). [b]BzMA = benzyl methacrylate, BMA = butyl methacrylate, TFEMA = 2,2,2-trifluoroethyl methacrylate, PEGMA = poly(ethylene glycol) methyl ether methacrylate, HEMA = 2-hydroxyethyl methacrylate, and DMAEMA = (dimethylamino)ethyl methacrylate. [c]Target degree of polymerization (DP) at 100% monomer conversion (calculated by $[monomer]_0/[R{-}I]_0$). [d]Addition of 10 wt% toluene (90 wt% monomer) for entries 1-4 and 6-10 and no addition of solvent (in bulk) for entry 5. [e]PMMA-calibrated GPC values. [f]Theoretical M_n calculated with $[monomer]_0$, $[R{-}I]_0$, and monomer conversion. [g]Molecular weight of monomer = 300. [h]PMMA-I is poly(methyl methacrylate)-iodide with M_n = 1900 and $Đ$ = 1.15. [i]PMMA-I with M_n = 3500 and $Đ$ = 1.12. [j]PPEGMA-I is poly(poly(ethylene glycol) methyl ether methacrylate)-iodide with M_n = 16000 and $Đ$ = 1.16.

Functional Methacrylates. The polymerization was amenable to a variety of functional methacrylates under both thermal (Table 2 (entries 1-7)) and photo conditions (Table 3 (entries 1-6)). The tables summarize the polymerizations of hydrophobic and hydrophilic methacrylates with benzyl (BzMA), butyl (BMA), lauryl (LMA), 2,2,2-trifluoroethyl (TFEMA), poly(ethylene glycol) (PEGMA), 2-hydroxyethyl (HEMA), and (dimethylamino)ethyl (DMAEMA) groups using the PPD-PO catalyst. Low-dispersity ($Đ$ = 1.13–1.49) polymers were obtained with high

conversions (70–95%) in all cases. These results clearly demonstrate the high monomer versatility of the PPD-PO catalyst.

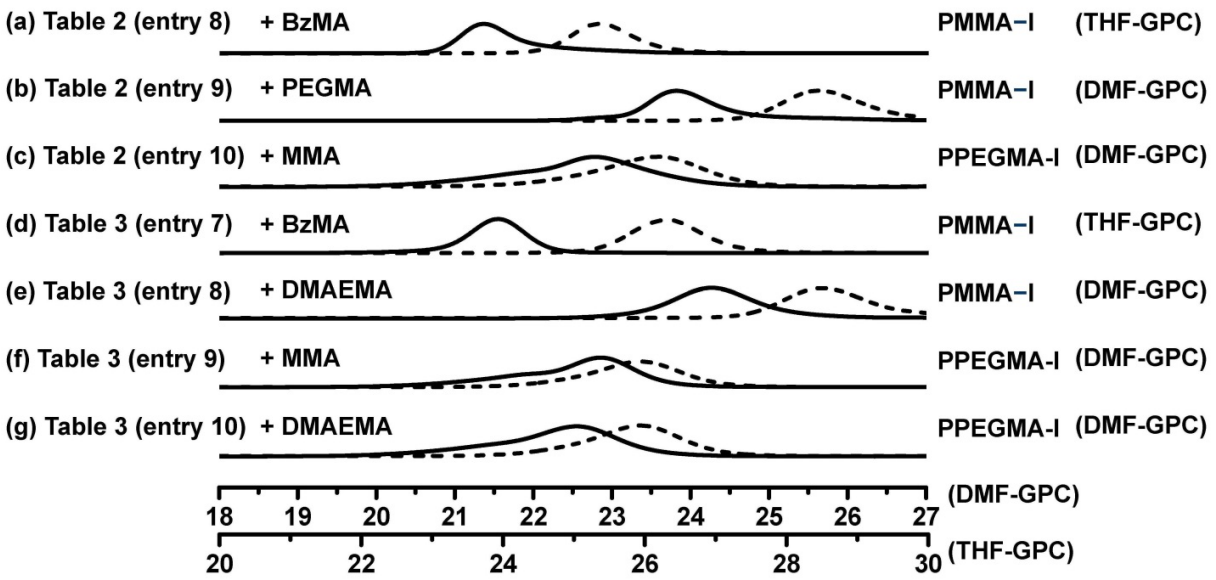

Figure 4. GPC chromatograms before (dashed lines) and after (solid lines) the block copolymerizations in Table 2 (entries 8-10) and Table 3 (entries 7-10).

Block Polymerizations. Exploiting the living character, we performed block polymerizations (Tables 2 (entries 8-10) and Table 3 (entries 7-10)). We synthesized macroinitiators under photo-irradiation because of the high iodide-chain-end fidelities. Using purified PMMA-iodide (PMMA–I) macroinitiators (M_n = 4700 and $Đ$ = 1.09 and M_n = 4200 and $Đ$ = 1.10), the thermal polymerizations of BzMA and PEGMA yielded hydrophobic-hydrophobic and hydrophobic-hydrophilic block copolymers, i.e., PMMA-*b*-PBzMA (M_n = 10000 and $Đ$ = 1.16) and PMMA-*b*-PPEGMA (M_n = 13000, $Đ$ =1.21) (Table 2 (entries 8 and 9)), where PBzMA is poly(benzyl

methacrylate) and PPEGMA is poly(poly(ethylene glycol) methyl ether methacrylate). A large fraction of the macroinitiator chains extended to block copolymers (Figures 4a and 4b), demonstrating the high block-efficiency. We also synthesized a PMMA-*b*-PPEGMA in the opposite order. Starting from a purified PPEGMA–I macroinitiator (M_n = 20000 and $Đ$ = 1.21), PMMA-*b*-PPEGMA (M_n = 32000 and $Đ$ = 1.36) was successfully obtained in the polymerization of MMA (Table 2 (entry 10) and Figure 4c). The photo polymerization was also effective for the second block (Table 3 (entries 7-10) and Figures 4d-4g), yielding PMMA-*b*-PBzMA, PMMA-*b*-PDMAEMA, PMMA-*b*-PPEGMA, and PPEGMA-*b*-PDMAEMA with low $Đ$ values (1.10-1.33), where PDMAEMA is poly((dimethylamino)ethyl methacrylate). These results demonstrate the applicability of this system to a range of block copolymer design, including hydrophobic-hydrophobic, hydrophobic-hydrophilic, and hydrophilic-hydrophilic block copolymers.

CONCLUSIONS

PO and PO derivatives efficiently catalyzed the generation of $R^{\bullet}$ from R-I and RCMP. A more electron-donating substitute led to a higher catalytic activity, as experimentally observed and theoretically supported. PPD-PO showed the highest catalytic activity and good solubilities in a range of monomers, are amenable to various functional monomers, and afforded well-defined block copolymers. The polymerization was induced and controlled by both thermal heating and photo irradiation using various PO catalysts. PO derivatives are easy to synthesize, which is attractive in tailored design of catalysts.

ASSOCIATED CONTENT

Supporting Information.

The Supporting Information is available free of charge on the ACS Publications Website at DOI: Experimental, chain-end analysis, analysis of a mixture of CP-I and PPD-PO, and DFT calculation sections (PDF)

AUTHOR INFORMATION

Corresponding Author

*E-mail: agoto@ntu.edu.sg

ORCID

Atsushi Goto: 0000-0001-7643-3169

Chen-Gang Wang: 0000-0001-6986-3961

Present Addresses

Division of Chemistry and Biological Chemistry, School of Physical and Mathematical Sciences, Nanyang Technological University, 21 Nanyang Link, 637371, Singapore.

Funding Source

This work was supported by Academic Research Fund (AcRF) Tier 2 from Ministry of Education in Singapore (MOE2017-T2-1-018).

Notes

The authors declare no competing financial interest.

REFERENCES

1. Desiraju, G. R.; Ho, P. S.; Kloo, L.; Legon, A. C.; Marquardt, R.; Metrangolo, P.; Politzer, P.; Resnati, G.; Rissanen, K. Definition of the Halogen Bond (IUPAC Recommendations 2013). *Pure Appl. Chem.* **2013**, *85*, 1711-1713.
2. Cavallo, G.; Metrangolo, P.; Milani, R.; Pilati, T.; Priimagi, A.; Resnati, G.; Terraneo, G. The Halogen Bond. *Chem. Rev.* **2016,** *116*, 2478-2601.
3. Mukherjee, A.; Tothadi, S.; Desiraju, G. R. Halogen Bonds in Crystal Engineering: Like Hydrogen Bonds yet Different. *Acc. Chem. Res.* **2014,** *47*, 2514-2524.
4. Priimagi, A.; Cavallo, G.; Metrangolo, P.; Resnati, G. The Halogen Bond in the Design of Functional Supramolecular Materials: Recent Advances. *Acc. Chem. Res.* **2013,** *46*, 2686-2695.
5. Gilday, L. C.; Robinson, S. W.; Barendt, T. A.; Langton, M. J.; Mullaney, B. R.; Beer, P. D. Halogen Bonding in Supramolecular Chemistry. *Chem. Rev.* **2015,** *115*, 7118-7195.
6. Goto, A.; Zushi, H.; Hirai, N.; Wakada, T.; Tsujii, Y.; Fukuda, T. Living Radical Polymerizations with Germanium, Tin, and Phosphorus Catalysts − Reversible Chain Transfer Catalyzed Polymerizations (RTCPs). *J. Am. Chem. Soc.* **2007,** *129*, 13347-13354.
7. Goto, A.; Suzuki, T.; Ohfuji, H.; Tanishima, M.; Fukuda, T.; Tsujii, Y.; Kaji, H. Reversible Complexation Mediated Living Radical Polymerization (RCMP) Using Organic Catalysts. *Macromolecules* **2011,** *44*, 8709-8715.
8. Goto, A.; Ohtsuki, A.; Ohfuji, H.; Tanishima, M.; Kaji, H. Reversible Generation of a Carbon-Centered Radical from Alkyl Iodide Using Organic Salts and Their Application as Organic Catalysts in Living Radical Polymerization. *J. Am. Chem. Soc.* **2013,** *135*, 11131-

11139.

9. Ohtsuki, A.; Lei, L.; Tanishima, M.; Goto, A.; Kaji, H. Photocontrolled Organocatalyzed Living Radical Polymerization Feasible over a Wide Range of Wavelengths. *J. Am. Chem. Soc.* **2015,** *137*, 5610-5617.
10. Wang, C. -G.; Goto, A. Solvent-Selective Reactions of Alkyl Iodide with Sodium Azide for Radical Generation and Azide Substitution and Their Application to One-Pot Synthesis of Chain-End-Functionalized Polymers. *J. Am. Chem. Soc.* **2017,** *139*, 10551-10560.
11. Wang, C.-G.; Hanindita, F.; Goto, A. Biocompatible Choline Iodide Catalysts for Green Living Radical Polymerization of Functional Polymers. *ACS Macro Lett.* **2018,** *7*, 263-268.
12. Matyjaszewski, K. Advanced Materials by Atom Transfer Radical Polymerization. *Adv. Mater.* **2018,** *30*, 1706441-1706462.
13. Matyjaszewski, K.; Tsarevsky, N. V. Macromolecular Engineering by Atom Transfer Radical Polymerization. *J. Am. Chem. Soc.* **2014,** *136*, 6513-6533.
14. Ouchi, M.; Sawamoto, M. Metal-Catalyzed Living Radical Polymerization: Discovery and Perspective. *Macromolecules* **2017,** *50*, 2603-2614.
15. David, G.; Boyer, C.; Tonnar, J.; Ameduri, B. Lacroix-Desmazes, P.; Boutevin, B. Use of Iodocompounds in Radical Polymerization. *Chem. Rev.* **2006,** *106*, 3936-3962.
16. Yamago, S. Precision Polymer Synthesis by Degenerative Transfer Controlled/Living Radical Polymerization Using Organotellurium, Organostibine, and Organobismuthine Chain-Transfer Agents. *Chem. Rev.* **2009,** *109*, 5051-5068.
17. Keddie, D. J.; Moad, G.; Rizzardo, E.; Thang, S. H. RAFT Agent Design and Synthesis. *Macromolecules* **2012,** *45*, 5321-5342.
18. Nicolas, J.; Guillaneuf, Y.; Lefay, C.; Bertin, D.; Gigmes, D.; Charleux, B. Nitroxide-

Mediated Polymerization. *Prog. Polym. Sci.* **2013**, *38*, 63-235.

19. Zetterlund, P. B.; Thickett, S. C.; Perrier, S.; Bourgeat-Lami, E.; Lansalot, M. Controlled/Living Radical Polymerization in Dispersed Systems: An Update. *Chem. Rev.* **2015,** *115*, 9745-9800.
20. Mastan, E.; Li, X. H.; Zhu, S. P. Destarac, M. Modeling and theoretical development in controlled radical polymerization. *Prog. Polym. Sci.* **2015**, *45*, 71-101.
21. Destarac, M. Industrial development of reversible-deactivation radical polymerization: is the induction period over? *Polym. Chem.* **2018,** *9*, 4947-4967.
22. Chen, M.; Zhong, M.; Johnson, J. A. Light-Controlled Radical Polymerization: Mechanisms, Methods, and Applications. *Chem. Rev.* **2016,** *116*, 10167-10211.
23. Goto, A.; Fukuda, T. Kinetics of Living Radical Polymerization. *Prog. Polym. Sci.* **2004,** *29*, 329-385.
24. Puttreddy, R.; Topić, F.; Valkonen, A.; Rissanen, K. Halogen-Bonded Co-Crystals of Aromatic *N*-oxides: Polydentate Acceptors for Halogen and Hydrogen Bonds. *Crystals* **2017,** *7*, 214-224.
25. Nizhnik, Y. P.; Sons, A.; Zeller, M.; Rosokha, S. V. Effects of Supramolecular Architecture on Halogen Bonding between Diiodine and Heteroaromatic *N*-Oxides. *Cryst. Growth Des.* **2018,** *18*, 1198-1207.
26. Łukomska, M.; Rybarczyk-Pirek, A. J.; Jabłoński, M.; Palusiak, M. The Nature of NO-Bonding in *N*-oxide Group. *Phys. Chem. Chem. Phys.* **2015**, *17*, 16375-16387.
27. Moad, G.; Rizzardo, E. Alkoxyamine-Initiated Living Radical Polymerization: Factors Affecting Alkoxyamine Homolysis Rates. *Macromolecules* **1995,** *28*, 8722-8728.
28. Wurz, R. P.; Lee, E. C.; Ruble, J. C.; Fu, G. C. Synthesis and Resolution of Planar-Chiral

Derivatives of 4-(Dimethylamino)pyridine. *Adv. Synth. Catal.* **2007**, *349*, 2345-2352.

29. Fischer, H. The Persistent Radical Effect: A Principle for Selective Radical Reactions and Living Radical Polymerizations. *Chem. Rev.* **2001**, 101, 3581-3610.
30. Chen, C.; Xiao, L.; Goto, A. Comprehensive Study on Chain-End Transformation of Polymer–Iodides with Amines for Synthesizing Various Chain-End Functionalized Polymers. *Macromolecules* **2016**, *49*, 9425-9440.
31. Sakashita, K.; Onuma, T.; Noda, T. Iron(II) Method for Converting Halogen Terminals of Methacrylic Acid Ester Polymers to Lactone Terminals. *Jpn*. Patent Application JP 2014015574, 2014.

For TOC only

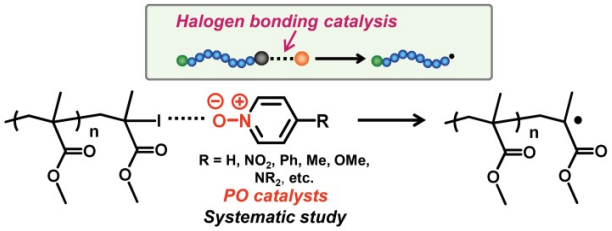
Halogen bonding catalysis
R = H, NO2, Ph, Me, OMe, NR2, etc.
PO catalysts
Systematic study